Nontopological solitary waves in continuous and discrete one-component molecular chains

Paweł Machnikowski,* Piotr Magnuszewski, and Andrzej Radosz
Institute of Physics, Wrocław University of Technology, Wybrzeże Wyspiańskiego 27, 50–370 Wrocław, Poland
(Received 23 June 2000; published 18 December 2000)

It is shown that the nontopological (bell-shaped) solitary waves in the asymmetric φ^4 model are unstable and correspond to saddle points of the potential energy of the continuous system. Their lifetime is estimated. In the discrete model, the potential energy landscape becomes rough: bell-shaped configurations may become stable. The potential energy function is analyzed around the bell-shaped configurations. A dynamical scenario for the decay of the metastable state in a discrete system, related to spontaneous energy localization, is shown.

DOI: 10.1103/PhysRevE.63.016601 PACS number(s): 05.45.Yv, 36.20.−r, 63.20.Ry

I. INTRODUCTION

Recent years have seen a revival of interests in the properties of molecular chains and of the systems comprising one-dimensional chains as an integral element of their structure. The latter group includes both the systems whose properties have been intensively studied, such as hydrogen bonded chains [1,2], on one hand and systems whose investigations have been much less extensive, such as polydiacetylenes [3,4] and DNA [5,6], on the other hand. Most of the attention is paid to their dynamical properties: from proton transport in hydrogen-bonded chains, via photoinduced structural phase transitions in polydiacetylenes, to the intriguing dynamics of DNA. In the course of careful examination of the dynamical properties of molecular chains an interesting issue has been brought to light: the characteristic feature that is common to all models is their *nonlinearity*. In hydrogen-bonded solid state systems, the proton is regarded as moving in a local bistable potential; in other systems such a local potential may have a periodic character. Usually, the dynamics of such systems was considered in the continuum limit, which seemed to be a reasonable and treatable approximation [7–11]. It was quite rich, accounting for both linear phonon excitation and nonlinear, localized kink excitations, or solitons. However, the dynamical properties of the real systems turn out to be much richer. Another important feature, apart from nonlinearity, that had to be taken into account is *discreteness* [8,12–16]. It is the interplay between the discreteness and the nonlinearity that has led to several interesting aspects of the dynamical behavior, localization of energy [17] being one of the most important.

In this paper, we discuss the dynamical properties of a one-dimensional, one-component system with a bistable, asymmetric potential. Such models have been used as an interpretation of various phenomena related to ferroelectric systems [2] and molecular chains appearing in living matter [18]. Metastable configurational states of such systems may be important for the conformational dynamics of the DNA macromolecule [19,20]. It has also been suggested [4] that the structural photoinduced phase transition [3] could be interpreted in terms of the model with an effective asymmetric double well potential.

In the continuum limit of the model under discussion, the only possible stationary, localized excitations in the absence of damping are nontopological, bell-shaped solitary waves [21,22]; when damping is present, stationary topological (kink) solutions moving at a constant speed may exist [21,23,24]. It was shown recently that the nontopological localized excitation is unstable [25]. It appears, however, that the discreteness would play a remarkable role here, which seems to be important due to possible experimental observations [26]. The key element of a structural transformation is the interplay between two energy parameters: one related to the local potential and the other one related to the strength of the nearest-neighbor interaction, the degree of discreteness. By removing the translational invariance of the continuous system, the discreteness affects, through the Peierls-Nabarro (PN) potential, the dynamics of localized-energy excitations. In the case of a symmetric double well potential, it results in a shifting of the frequency of the Goldstone-like excitation, $\omega_G^2 > 0$. Therefore, one might expect that in the case of an asymmetric potential, the discreteness might also shift the frequency of the fluctuations around a localized-energy excitation, which might result in stabilizing the bell shape. This would lead to interesting consequences for photoinduced structural changes and for their possible future applications. These aspects of the discrete systems with a bistable asymmetric potential have been the main motivation for the studies, the results of which are presented below.

In the following section, we study the stability properties of the nontopological excitation in the continuum limit. The dynamics of the collapse of the bell-shaped configuration is discussed. In Sec. III we describe the influence of the discreteness on the possible stable configurations of the system. We also examine in detail the structure of the potential energy around the discrete bell-shape-like configuration. Next, we show that discreteness may lead to a new scenario of metastable state decay. Section IV contains a discussion of the results.

II. NONTOPOLOGICAL SOLITARY WAVE AND ITS STABILITY

Let us consider the properties of the continuous nonlinear Klein-Gordon (φ^4) system defined by the Hamiltonian

*Email address: machnik@if.pwr.wroc.pl

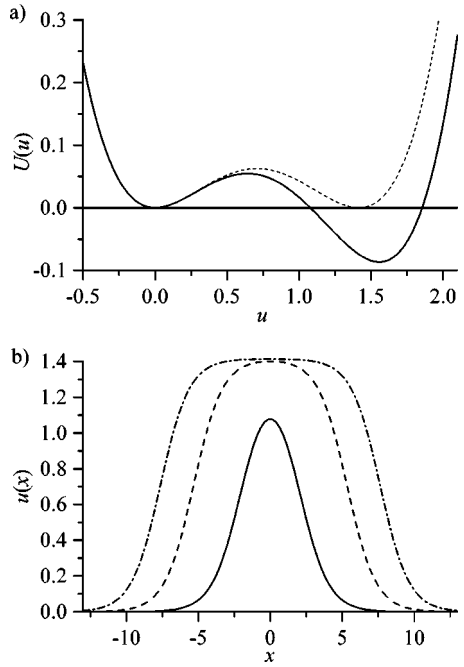

FIG. 1. Asymmetric potential (in dimensionless units) (a) and corresponding bell-shape solution (b). Plots correspond to $B=2.2 \approx B_0+7\times10^{-2}$ (solid line), $B=B_0+10^{-4}$ (dashed lines), and $B=B_0+10^{-6}$ [dash-dotted lines; indistinguishable from the previous one in (a)].

$$H=\int dx\left[\frac{1}{2}\dot{u}^2(x,t)+\frac{1}{2}u'^2(x,t)+U[u(x,t)]\right], \qquad (1)$$

where

$$U(u)=\frac{1}{2}u^2-\frac{B}{3}u^3+\frac{1}{4}u^4. \qquad (2)$$

When $B=B_0=3/\sqrt{2}$ the potential has two degenerate minima at $u=0$ and $u=1/(\sqrt{2})$. We will focus on the case $B>3/\sqrt{2}$, in which the potential has two nondegenerate minima: a local one for $u=0$ and the absolute one at $u=u_{\min}=(B+\sqrt{B^2-4})/2$ [see Fig. 1(a)].

The dynamical equation obtained from the Hamiltonian (1) is

$$\ddot{u}-u''+u^3-Bu^2+u=0, \qquad (3)$$

where the dots and primes denote differentiation with respect to t and x, respectively.

The only nontrivial stationary (''traveling'') solution to the Lorentz-invariant equation (3) is the nontopological, bell-shaped solitary wave [22]

$$u_{\rm b}(x,t)=\frac{a}{b+\cosh[\gamma(x-vt)]}, \quad -1<v<1, \qquad (4)$$

where $a=3/[B^2-B_0^2]^{-1/2}$, $b=aB/3$, $\gamma=[1-v^2]^{-1/2}$. The form of this solution is presented in Fig. 1(b).

It is clear that the energy of the bell-shape solution is higher than the energy of both the metastable state, $u\equiv0$, and the globally stable state, $u\equiv u_{\min}$. Since the bell shape is a nontopological solution, it may be continuously deformed to any of these two states. Therefore, it should not be expected to be stable [27,28]. To verify this, let us follow the standard linear stability analysis [9,27]. Writing in the bell shape's resting frame, $\zeta=\gamma(x-vt)$, $s=\gamma(x+vt)$,

$$u(\zeta,s)=u_{\rm b}(\zeta)+\phi(\zeta)e^{i\lambda s}, \qquad (5)$$

the equation of motion (3) linearized in ϕ takes the form of a Schrödinger-like eigenvalue problem

$$-\partial_\zeta^2\phi(\zeta)+V(\zeta)\phi(\zeta)=\lambda^2\phi(\zeta), \qquad (6)$$

where

$$V(\zeta)=\left[\frac{d^2U(u)}{du^2}\right]_{u=u_{\rm b}(\zeta)}=3u_{\rm b}^2(\zeta)-2Bu_{\rm b}(\zeta)+1. \qquad (7)$$

The characteristic feature of the spectrum of the operator

$$-\partial_\zeta^2+V(\zeta) \qquad (8)$$

corresponding to localized energy excitations in continuous systems is the presence of the zero-frequency mode, $\lambda=0$. The appearance of such a mode accompanies the broken continuous symmetry—the translational invariance. However, this broken symmetry is not an internal one and instead of a Goldstone, gapless mode, one gets a separated, zero-frequency excitation, hereafter called a pseudo-Goldstone mode. In the system with a symmetric potential, $B=B_0$, the localized energy excitation is the kink (or antikink) solution,

$$u_{\rm k,ak}(\zeta)=\frac{1}{\sqrt{2}}\left(1\pm\tanh\frac{\zeta}{2}\right), \qquad (9)$$

and $V(\zeta)$ in Eq. (6) takes the form of the Pöschl-Teller (PT) potential [7,29]

$$V(\zeta)\ \overset{B\to B_0}{\rightarrow}\ V_{\rm K}(\zeta)=1-\frac{3}{2}\cosh^{-2}\frac{\zeta}{2}. \qquad (10)$$

The discrete spectrum of this potential consists of the ground level $\lambda_0^2=0$, whose eigenfunction is the translational symmetry-restoring mode $\partial_\zeta u_{\rm k,ak}$, and an excited level $\lambda_1^2=3/4$ [30,31].

In the case of an asymmetric potential, $V(\zeta)$ is defined by Eq. (7) and the function $\phi_{\rm G}(\zeta)=\partial_\zeta u_{\rm b}(\zeta)$ corresponds to the pseudo-Goldstone excitation but it has one node. Therefore, it is related to the (first) excited level, $\lambda_1^2=0$, and there must be a ground state solution of Eq. (6), a nodeless one, belonging to a lower eigenvalue, $\lambda_0^2<0$. Such a solution, having imaginary frequency [cf. Eq. (5)], explodes exponentially, destroying the original solution. The magnitude $|\lambda_0|^{-1}$ may be interpreted as the lifetime of the bell-shaped solitary wave.

In a weakly asymmetric system, $B\to B_0$, the bell-shaped solution has a wide kink-antikink-like form. The potential $V(\zeta)$ is composed of two Pöschl-Teller wells (10) separated

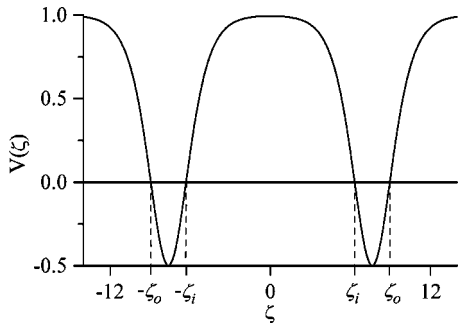

FIG. 2. Potential for stability analysis for almost degenerate minima of the on-site potential, $B=B_0+10^{-6}$.

by a wide barrier (Fig. 2). In effect, the two discrete eigenvalues of the potential $V_K(\zeta)$ become split. Due to the translational symmetry of the system, the ground level is split in such a way that the eigenvalue $\lambda_1^2=0$ is retained, but now related to the excited level. The negative eigenvalue λ_0^2 may be found in this limit by semiclassical methods. The quantitative calculation (see the Appendix) leads to the following formula for the bell shape's lifetime:

$$|\lambda_0|^{-1}\approx 2\sqrt{\frac{3\pi}{7+4\sqrt{3}}}\frac{1}{\sqrt{B^2-B_0^2}}e^{0.9}.$$

The other localized state of the Pöschl-Teller potential produces in the same way a pair of positive eigenvalues related to two real-frequency modes around the bell shape. (Note the analogy between the above analysis and that of the double-Morse potential treated as two Morse wells separated by a certain, variable distance [32].)

In the opposite limit, when $B\to\infty$, the potential $V(\zeta)$ has again the Pöschl-Teller form, but with different parameters,

$$V(\zeta)\overset{B\to\infty}{\to}V_\infty(\zeta)=1-3\cosh^{-2}\frac{\zeta}{2},$$

and $\lambda_0=-\sqrt{5}/2$, hence $|\lambda_0|^{-1}\to 2/\sqrt{5}$ [30,31]. In this limit there is one positive frequency mode, $\lambda_2^2=3/4$.

Figure 3 shows $|\lambda_0|^{-1}$ obtained by numerical methods for various values of B. As may be seen, it decays very fast to the asymptotic value of $2/\sqrt{5}$. This lifetime should be compared to the characteristic time scales of the system. For instance, the period of phononic oscillations ranges from $2\pi/\sqrt{5}$ to 2π. Also, the velocities of the nonlinear excitations are lower than 1. Hence, the bell shape can travel during its lifetime only the distance of less then one node. Thus, the lifetime of this nonlinear excitation is very short, except for nearly symmetric potentials, where the bell shape actually consists of a pair of nearly independent kinks fairly distant from each other (cf. Fig. 1).

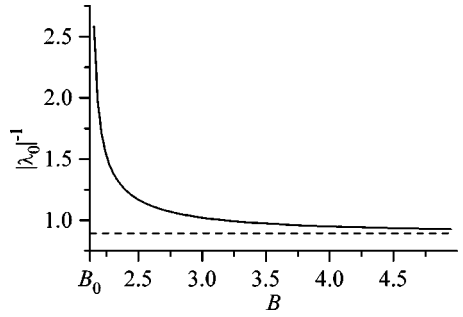

FIG. 3. Lifetime of the bell-shaped solitary wave for various values of asymmetry between minima of the on-site potential (determined by the parameter B). Dashed line shows the asymptotic value of $2/\sqrt{5}$.

The above results indicate that the resting bell-shaped configuration is a saddle point in the potential energy landscape of the system. The potential energy function around this configuration has negative curvature in exactly one direction (corresponding to the negative eigenvalue) and zero curvature in another direction, related to the translational mode.

It is obvious that an excitation appearing in a real system is unlikely to be exactly of the form (4). The unavoidable discrepancy (however small it is) will lead to the collapse of the configuration. Further system dynamics depends on the direction of the collapse towards the local or global minimum. In the former case the bell shape turns into a localized oscillatory excitation living on the false vacuum state. Such excitations might be absolutely stable only in a discrete system [33,34]. However, even in a continuous one their lifetimes prove to be very long. This fact may be qualitatively understood by noticing that the frequency of oscillations is very low for such large-amplitude motion (the dynamics originates at the saddle point and is still close to the separa-

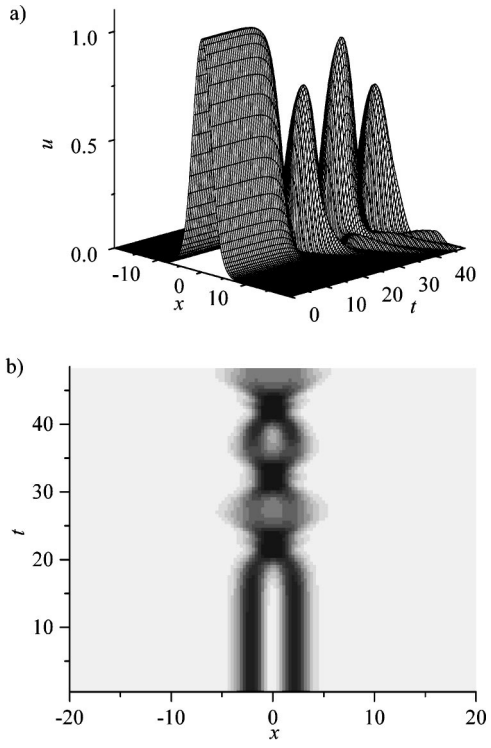

FIG. 4. System dynamics ($B=2.2$) after collapse of a bell shape to the false vacuum state; (a) system configuration, (b) energy density.

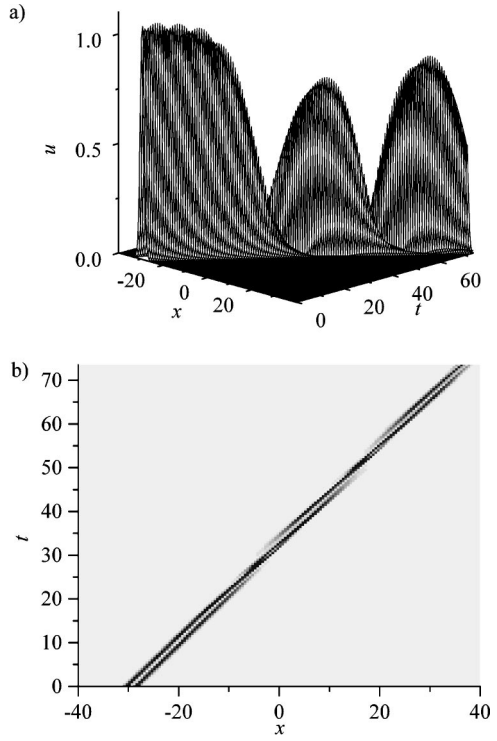

FIG. 5. System dynamics ($B=2.2$) after collapse of a bell shape to the false vacuum state with an initially moving bell shape. (a) System configuration, (b) energy density.

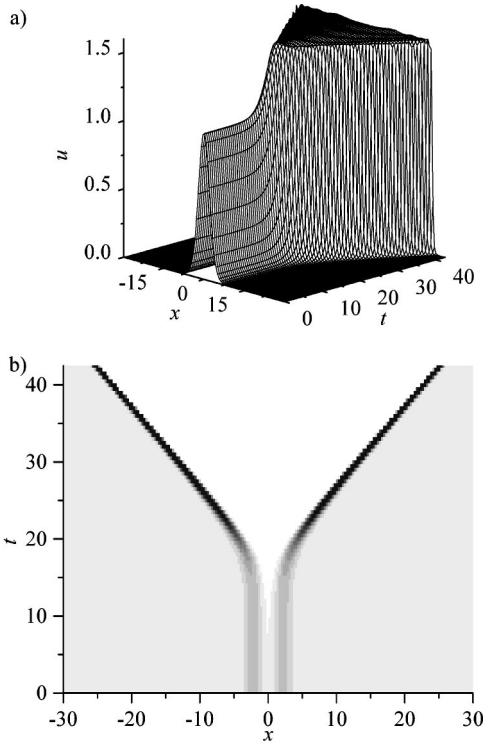

FIG. 6. System dynamics ($B=2.2$) after collapse of a resting bell-shape to the true vacuum state. (a) System configuration, (b) energy density.

trix). Thus, only the relatively weakly excited second harmonic enters into the phonon spectrum and, moreover, it is located far above its lower edge, i.e., in a region of low density of phonon states. For these reasons, radiation is rather weak and the system remains for a relatively long time in the oscillating state (Fig. 4). This kind of dynamics is similar to the bubble collapse leading to long-living spherically-symmetric ''oscillon'' states in three-dimensional theories [35–37]. A large bubble may easily be excited, either by external interaction or by internal dynamics, and the system may pass through the saddle towards the global minimum (see Sec. III C).

When the initial system state is a moving bell shape, the bubble resulting from its collapse moves with the same velocity (Fig. 5) which, in fact, results from the Lorentz invariance of the problem. After the collapse towards the global minimum, the bell-shape state splits into two kinks traveling towards system ends (Fig. 6) [38]. In the presence of damping, a kink in an asymmetric potential moves with a certain constant speed [23]. Since there is no explicit damping in the system, kinks may be expected to accelerate to the speed of sound ($v=1$). However, some energy loss takes place due to radiation (also because of discretization unavoidable in simulation), leading to stationary movement with a speed very close to $v=1$. It is interesting to note that both kinks move with the same speed, irrespective of the original bell-shape velocity (Fig. 7). This does not violate conservation laws, since fast kinks have high energy and even very slight and unnoticeable velocity differences lead to sufficient asymmetry in momentum. Moreover, some momentum may be transferred to radiation.

III. DISCRETENESS EFFECTS

In this section, we will consider the dynamical properties of the discrete version of the system (1). In this case, the Hamiltonian takes the form

$$H=\sum_n \left[\frac{1}{2}\dot{u}_n^2(t)+\frac{1}{2}\kappa[u_{n+1}(t)-u_n(t)]^2+U[u_n(t)]\right] \qquad (11)$$

and the equation of motion (3) is now replaced by the system of equations

$$\ddot{u}_n-\kappa(u_{n+1}-2u_n+u_{n-1})+u_n-Bu_n^2+u_n^3=0. \qquad (12)$$

Discreteness eliminates the translational invariance of the system, leading to serious modification of both stability conditions and system dynamics. There are three essential effects related to discreteness: (i) the appearance of local minima of the potential energy corresponding to bell-shape-like states for high enough discreteness; (ii) the complex structure of saddle points of the potential energy replacing the translationally invariant bell-shape solution; (iii) modification of the system dynamics due to the existence of discrete breathers [34] and discreteness effects on the kink dynamics, well known from symmetric systems [8].

A. Local minima

In the limit of independent oscillators ($\kappa\to 0$) any configuration with some nodes in the right well and the rest in the left well is stable. In particular, any bell-shape-like con-

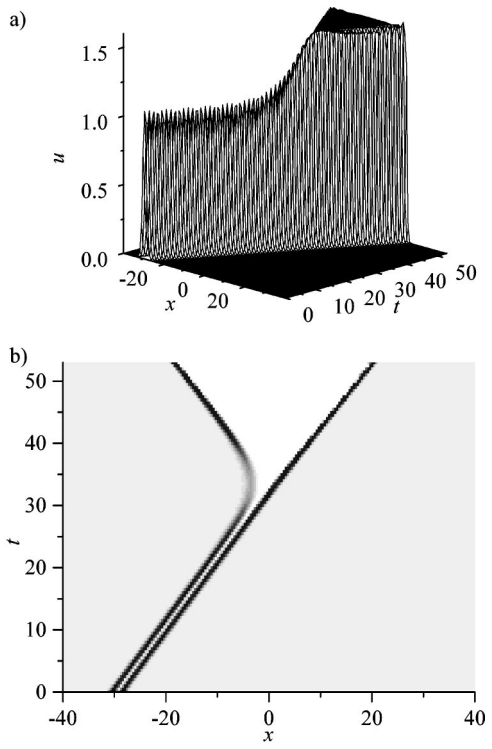

FIG. 7. System dynamics ($B=2.2$) after collapse of a bell shape moving with initial velocity $v=0.9$ to the true vacuum state. (a) System configuration, (b) energy density.

figuration, i.e., one with a certain number of consecutive nodes placed exactly in the global minimum, is stable. One may expect that for low values of κ all these configurations survive in a slightly changed form. They will gradually become unstable when the value of κ is increased. Figure 8 shows one of the stable solutions of Eq. (12). Note that the central node lies closer to the global minimum than the corresponding part of the continuous system. For each value of B one finds the critical value of κ below which such a one-node configuration is stable. Continuing this type of procedure, one can identify the area of stability of the two-node configuration, three-node configuration, etc. The final result is presented in Fig. 9: below the nth consecutive line in the B-κ frame, the corresponding n-node configuration is stable. Note that for any n there is an area of parameters where only the n-node configuration is stable.

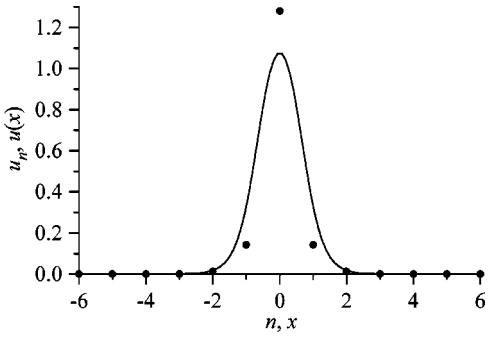

FIG. 8. Stable system configuration corresponding to a bell shape.

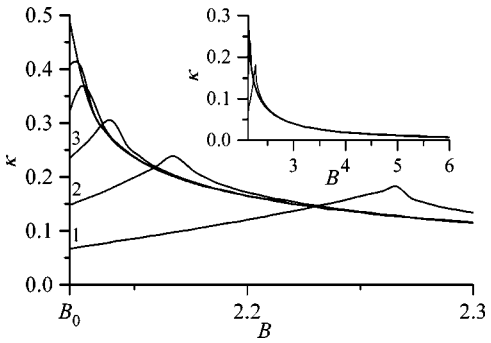

FIG. 9. Stable configurations of a discrete system (see explanation in text). Inset shows the diagram for a wider range of B.

The existence and disappearance of the stable configurations is related to the restructuring of the phonon modes around them. As we have seen, in the continuum limit there is one growing, imaginary-frequency mode, one zero-frequency Goldstone mode, and a certain number of periodic (real-frequency) localized modes. The behavior of such modes was examined for kinklike equilibria in symmetric potentials where only the Goldstone mode and periodic modes exist. It is known that the former moves up and transforms in a periodic Peierls-Nabarro mode related to oscillations of the pinned kink around its equilibrium position in the PN potential [39]. The higher modes are related to shape-changing oscillation of the kink. Stabilization of a bell-shaped excitation in a discrete system means that not only the Goldstone mode has become a nonzero real-frequency mode, but so has the exploding mode. Due to their topology, the former now corresponds to the PN mode (oscillation of the bell-shaped excitation as a whole) and the latter is a kind of a shape mode. The structure of localized modes as a function of discreteness and asymmetry is shown in the Fig. 10.

It must be noted that the stability of a discrete bell-shape-like configuration has only local character, i.e., it may be destroyed by large enough perturbations. Moreover, discrete configurations obviously correspond only to resting bell-shaped excitations.

B. Saddle points

For many applications it is essential to know the quantitative properties of the potential energy landscape around the saddle point separating the globally stable state from the metastable state. This problem, trivial in the continuum case (a continuous family of saddle-point configurations related by translation) becomes much more complicated when discreteness is taken into account.

First, one needs a procedure for searching for the saddle points of the potential energy. It is essential to note that we are interested in finding the closest characteristic point ($\nabla E_{\mathrm{pot}}=0$) rather than the global minimum (which is trivial) or maximum (which does not exist). A suitable method consists in approximating the potential energy function at the starting point by its second order series expansion and going to the saddle point of the obtained function which then becomes the starting point for the next iteration.

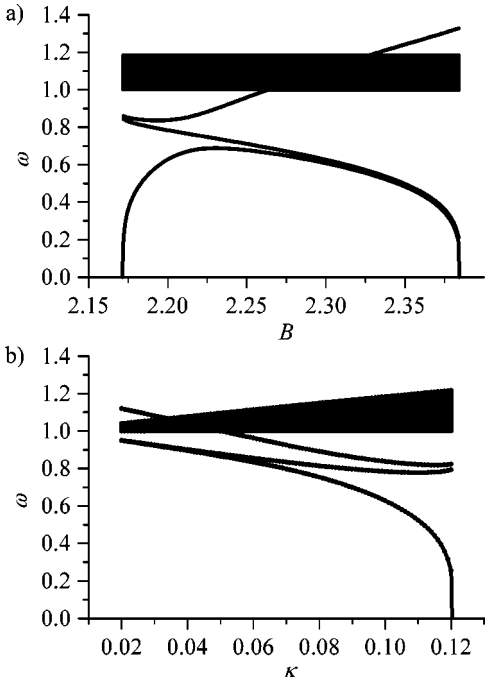

FIG. 10. Linear modes (localized and extended) around the one-node configuration; (a) as a function of B for $\kappa=0.1$, (b) as a function of κ for $B=2.2$.

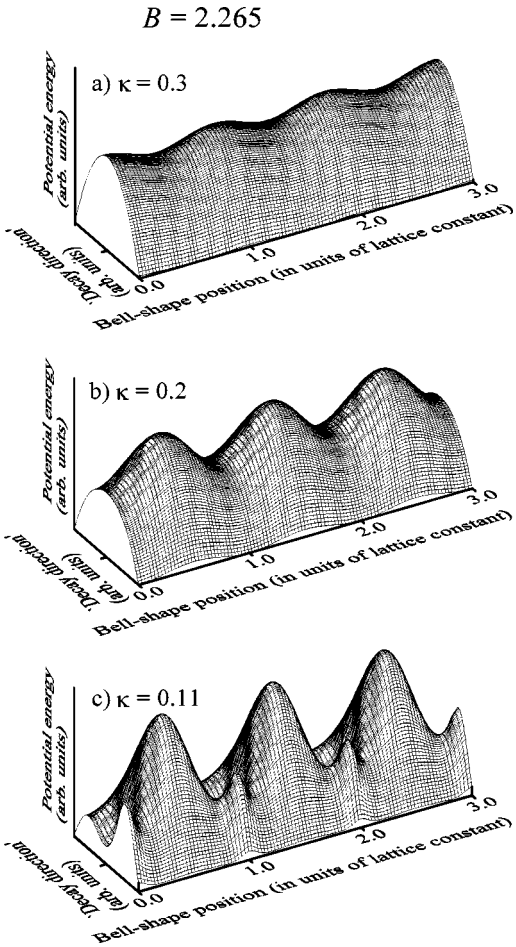

FIG. 11. Schematic plot of the potential energy around the bell-shaped configurations in the discrete system for $B=2.265$. The plots refer to two directions, one related to the exploding mode and the other one related to the formerly translational mode.

As a first example, let us take the value of $B=2.265$, corresponding to the rightmost peak in Fig. 9. The schematic plot of the potential energy function is shown in Figs. 11(a)–11(c). There are no stable bell-shaped configurations for strongly coupled chain, $\kappa>0.18$ and only saddle configurations are possible. For $\kappa>0.603$ there is a series of saddle points corresponding to bell-shaped configurations centered on the nodes of the chain. At these saddle points the potential energy function has exactly one negative curvature and they will be referred to as *proper saddles*. Somewhere between any two adjacent proper saddles there is always a characteristic point with two negative curvatures (a double-saddle point). It has a higher energy than the proper saddle. One may think of it (not strictly) as a transition from one proper saddle configuration to the neighboring one (which means shifting the bell shape by one node) along a ridge; between two saddles there must be a hill. This description obviously refers only to the two selected directions corresponding to the collective coordinates of the system. One of them is the size of the bell shape and is related to the exploding mode and the other one is the position along the system and is related to the formerly translational mode. All the other ''directions'' correspond to positive curvatures.

As κ decreases, the roles of the proper saddles and ''pseudohills'' (double-saddle configurations) are interchanged at $\kappa=0.603$ and then again at $\kappa=0.213$—the proper saddles may correspond to configurations centered on or between the nodes. The first two plots in Fig. 11 correspond to these two different situations.

The relative difference between energies of these saddle point configurations, normalized to the lower one, are plotted in the Fig. 12(a). Note that the energy difference may be considerable compared to the total energy of the saddle-point configuration. For high values of κ the second lowest curvature gradually diminishes for both types of saddle points and so does the energy difference between them. In this way, the translational symmetry of the continuum limit appears.

Below the value $\kappa\approx0.18$ the one-node configuration becomes a local minimum and there is a double-saddle point corresponding to the two-node configuration separating the equivalent minima related by shifting the configuration by one lattice spacing [Fig. 11(c)].

It is evident from Fig. 9 that below $\kappa\approx0.13$ many local minima appear; however, all of them are located far from the ''ridge'' and their energies are very low. The potential energy landscape for such a discrete system becomes very complex and cannot be described in terms of the two-dimensional space of collective coordinates. Actually, as the discreteness grows, the system undergoes a transition from the collective decay scenario to the individual one.

For a weakly coupled chain a reduced system approximation is useful [34,40], in which only two nodes are allowed to move, while the others are fixed at the local minimum. The potential energy of such a system for various values of κ is plotted in the Fig. 13. The figures show also the lowest en-

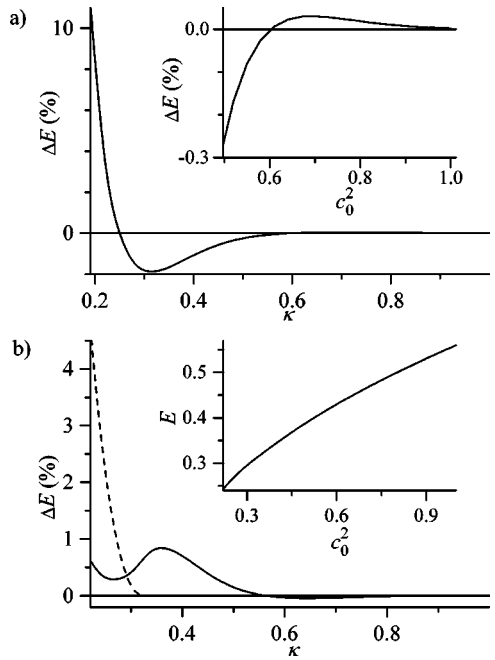

FIG. 12. Comparison of energies of different saddle-point configurations, (a) $B=2.265$. The main plot shows the relative energy difference, $\Delta E=(E_{1/2}-E_1)/\min(E_{1/2},E_1)$, between the saddle point configurations centered on a node and between nodes. The inset shows the same for a wider range of κ. (b) $B=2.158$. Main plot, solid line shows the relative energy difference, $\Delta E=(E_{1/2}-E_1)/\min(E_{1/2},E_1)$, between the saddle point configurations centered on a node and between nodes. Main plot, dashed line shows the relative energy difference, $\Delta E=(E_1-E_{1/3})/E_{1/3}$, between the saddle point at $n=1/3$ and the on-node saddle-point configuration. Inset shows the total, absolute energy of the saddle (with respect to the metastable minimum).

ergy paths joining the two deepest minima. For uncoupled nodes, $\kappa=0$, [Fig. 13(a)] it is clear that the path corresponds to first shifting one of the particles over the hump and then doing the same with the other one. As the value of κ increases [Figs. 13(b)–13(c)], the nodes move in a more collective way: shifting one node requires some displacement of the other one. Nonetheless, the second node still undergoes only a slight displacement until the first node is placed in the deeper minimum. In the context of the full chain this corresponds to the fact that in a strongly discrete chain the ''cheapest'' way is to move the nodes over the hump one by one.

The second example corresponds to $B=2.158$. For this value of B various kinds of configurations stabilize almost simultaneously (see Fig. 9) leading to the appearance of many local minima at $\kappa\approx 0.218$.

Let us start the discussion close to the continuum limit, as previously. For $\kappa>0.56$ there is a proper saddle point centered in between the nodes and a double-saddle point centered on a node. The relative difference between the potential energy at these points is very low: e.g., for $\kappa=0.7$ its value is 3.2×10^{-4} of the potential energy barrier height [Fig. 14(a)]. The solution is very similar to the continuum one and the number of nodes involved in the configuration grows with κ.

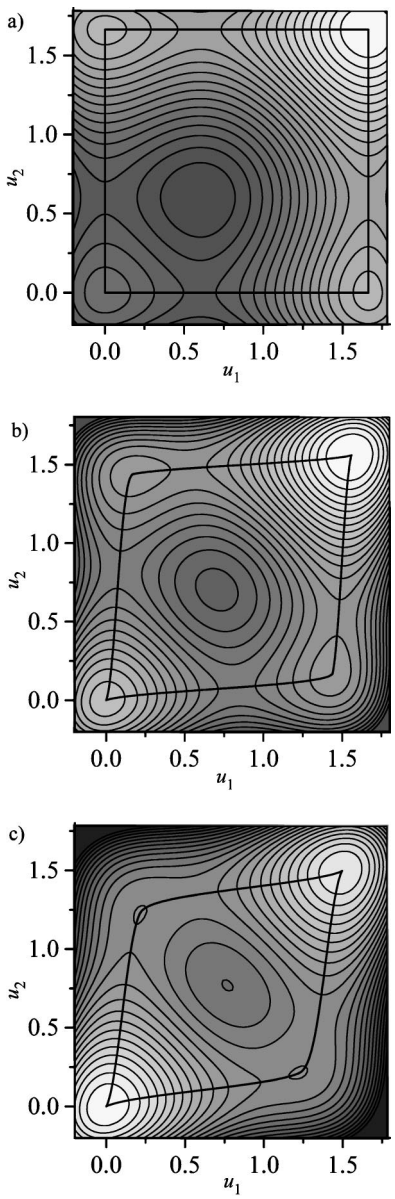

FIG. 13. Potential energy of a reduced, two-node system for $B=2.265$ and (a) $\kappa=0$, (b) $\kappa=0.1$, (c) $\kappa=0.15$. The thick line shows the lowest energy paths joining the two local minima.

For $0.32<\kappa<0.56$ the roles of the characteristic points switch [Fig. 14(b)]. The on-node configuration (three nodes) now corresponds to the proper saddle. For $\kappa\approx 0.322$ the proper saddle bifurcates into a double saddle located on a node and a proper saddle separating it from the double saddle located in between the nodes [Fig. 14(c)]. The proper saddles are shifted by approximately 1/3 of the lattice spacing from the on-node configuration which means that they correspond to asymmetric configurations. Figure 12(b) compares energies of different saddle points.

The almost simultaneous appearance of many local minima at $\kappa\approx 0.218$ causes the potential energy to become very flat at many points. Below this critical value there are local minima corresponding to many different kinds of configurations centered both on a node and between nodes (out of them, the two- and three-node configurations have the

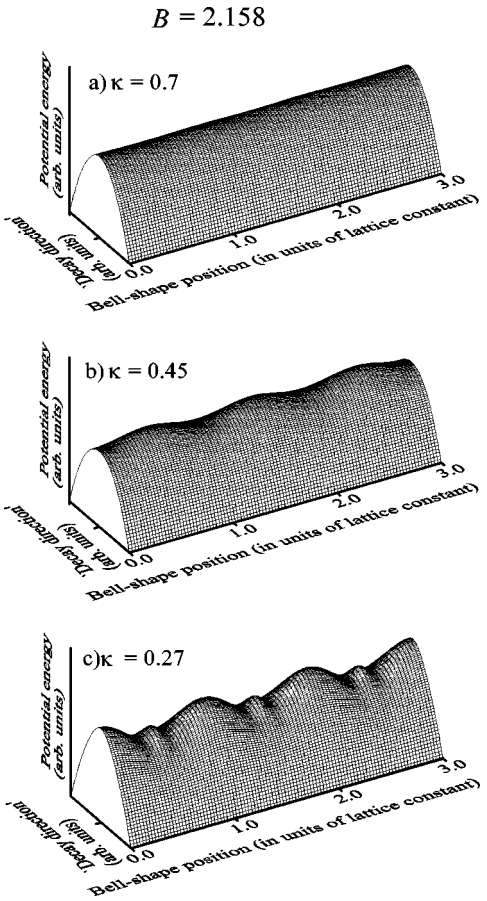

FIG. 14. Schematic plot of the potential energy around the bell-shaped configurations in the discrete system for $B=2.158$. The plots refer to two directions, one related to the exploding mode and the other one related to the formerly translational mode.

highest energies, i.e., are the closest to the barrier). It is impossible to present the potential energy of the system in a collective coordinates diagram.

The above examples reveal that the potential structure of a discrete chain in a double-well potential strongly depends on the system parameters. For small discreteness (higher values of κ) the most important effect is the overall lowering of the saddle compared to the continuum approximation [see the inset in Fig. 12(b)]. But when the nearest-neighbor coupling weakens, the physical properties of the system will be affected by the growing roughness of the potential energy landscape. Below a certain value of κ there is no point in speaking about bell-shaped (collective) configurations. Instead, the system should be described in terms of the individual dynamics of the nodes.

C. Dynamical effects characteristic of discrete systems

Discreteness is also important for the system dynamics after the collapse of the bell-shaped configuration. In view of the large lifetimes of oscillatory states, for the collapse towards the local minimum the difference may be seen only on very large time scales and consists in stopping the decay of the bubble at a certain stage and converting it into stable discrete breathers.

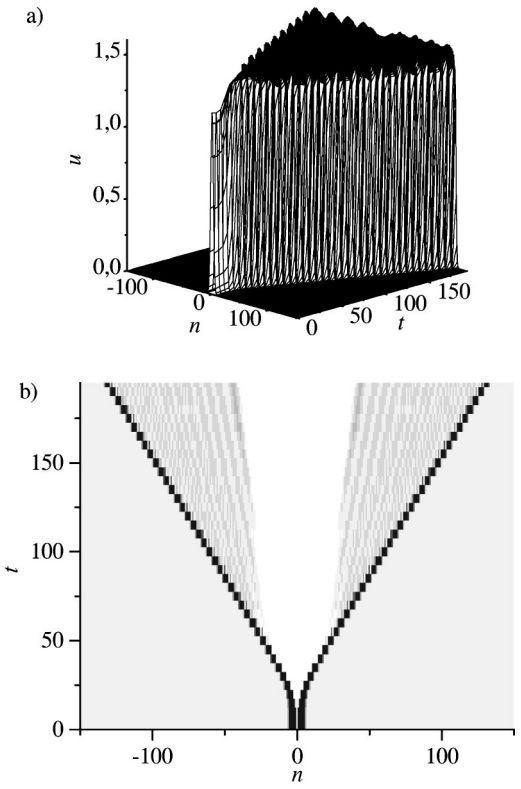

FIG. 15. Collapse of the bell-shaped configuration in a discrete system. Due to radiation effects, the kinks speed is lower than $\sqrt{\kappa}$.

On the other hand, when the bell-shaped excitation collapses into an expanding sector (bubble) of globally stable state, discreteness modifies considerably the kink dynamics. Due to radiation [8,39], the kink motion is effectively damped and its speed stabilizes at some value $v<\sqrt{\kappa}$. An example is shown in Fig. 15, where the kinks originating from a collapse of a bell-shaped configuration move with a constant velocity of $v\approx 0.75\sqrt{\kappa}$. Hence, the effect of discreteness on bubble expansion is similar to that of thermal noise [38].

Since the bell-shaped configuration is a saddle point of the potential energy, the decay of the metastable state must be initiated by the formation of a ''bubble'' larger than the bell-shaped configuration. From the usual thermodynamical point of view, this might occur only in the presence of thermal fluctuations. The theory behind such decay is now well understood [41–43]. However, when the mean energy (temperature) is low, a large enough fluctuation is extremely improbable.

In a discrete system, even an isolated one, processes of spontaneous energy localization take place [17]. Such processes lead to formation of discrete breathers that are very long-lived and have relatively large (although limited) amplitudes and energies. Small (''light'') breathers may move along the system, while large (''heavy'') ones can only be resting [44].

During collisions, larger breathers tend to grow at the expense of smaller ones [17], until they reach the maximum possible size. This size is determined by the requirement that the second harmonic of the breather frequency lie above the

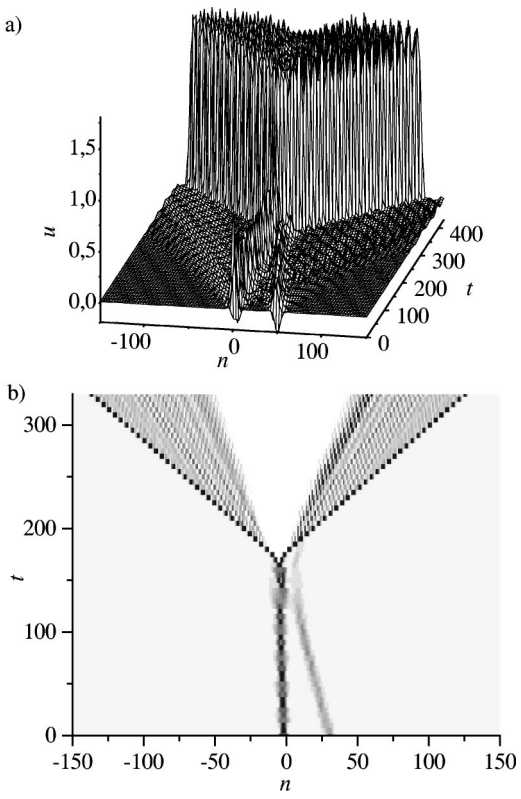

FIG. 16. An example of dynamical decay of the metastable state due to two-breather collision.

phonon spectrum [45,34]. If there were breathers close to the critical size (i.e., such that further increasing the amplitude would overthrow the system towards the global minimum), their frequency would be close to 0, contradicting the above requirement. Hence, the largest breather must have lower energy than necessary to pass through the saddle.

However, collisions between breathers may lead to the following scenario: a small moving breather collides with a large (resting) one; the total energy is large enough and the system crosses the saddle point (or, strictly speaking, it crosses the potential energy ridge at a certain point, not necessarily at the saddle) and an expanding critical bubble originates. An example of such a dynamical decay process is shown in Fig. 16.

A criterion for a possibility of a dynamical (as opposed to thermodynamical) decay scenario is roughly as follows: the total energy of the largest possible resting breather together with the largest possible moving one should exceed the saddle point height (over the false vacuum configuration) which is equal to the bell-shape energy.

At low temperatures this dynamical process may strongly contribute to the probability of the decay of the metastable state. However, the statistical properties of breather formation seem to be understood insufficiently to allow any quantitative conclusions. It is important to note that we neglect any quantum effects that would lead to a completely different decay mechanism (tunneling instead of thermally activated) for low temperatures [42].

IV. CONCLUSIONS

We have studied the properties of nontopological, bell-shaped excitations in both continuum and discrete systems with asymmetric on-site potentials. We have shown that such excitations in the continuum model are unstable. The lifetime of the bell-shaped waves has been estimated in the two limiting cases: strong asymmetry and weak asymmetry. The short lifetime of these excitations prevents them from having any importance for the transport phenomena.

The collapse of a bell-shaped wave may lead either to a slowly vanishing oscillating bubble excitation around the local minimum of the system or to an expanding sector of the system lying in the global minimum. This sector is bounded by two kinks moving (in the continuum case) with the speed of sound. The analogy with three-dimensional systems discussed elsewhere [36–38] seems interesting here.

The bell-shaped configuration of the continuous system is a saddle point of the potential energy. Actually, due to the continuous translational symmetry there is a family of equivalent saddle points. Through these saddle points the decay of the metastable state of the system is most likely to happen.

In the discrete system the potential energy around the configurations analogous to the continuum bell shapes becomes rough. For systems close to the continuum limit this roughness consists simply in replacing the original continuum of equivalent saddle points with isolated saddle points separated by ''hills'' (saddle points with two negative curvatures). This might seem analogous to the Peierls-Nabarro potential for kinks but unlike the latter, the potential energy for bell-shaped waves cannot be rigorously defined and has not much importance, since such waves are not stable. For strongly discrete systems, the shape of the potential energy becomes essentially different: many saddle points and local minima may appear. These characteristic points may be numerically searched out and classified but a clear picture may be obtained only for the most discrete systems where the approximation by a reduced system with two degrees of freedom is applicable. One may conclude that with growing discreteness the system undergoes a crossover from the collective decay path (metastable state decay is likely to involve the formation of a bell-shaped saddle-point configuration) to the single-node path (the nodes move to the global minimum one by one)—domino effect [4].

Discreteness leads also to new effects during the collapse of a bell-shaped configuration: the decay of the oscillating bubble may be stopped by forming a discrete breather and the kinks bounding the expanding sector move with lower velocity.

An interesting generalization of the results presented in this paper would be to include the two-component systems. It was shown [46] that in a two-component model, where the system (1) is coupled in a special way to another, harmonic Klein-Gordon field, the equations of motion may be reduced to a one-component problem and solved (see also [47]). However, it may be shown (see [25]) that such an excitation is unstable, at least for low velocities. This property should be contrasted with the stability of excitations (kink with accompanying bell shape) in symmetric models [1].

Another interesting idea was proposed by Volkov [20] who constructed a model in which the asymmetric on-site potential is generated dynamically. Such a system supports only moving bell-shaped waves. Their stability cannot be rigorously examined due to the lack of Lorentz invariance (cf. [25]). They might be expected to be unstable: except for the collapse, similar to that described in this paper, Volkov's solitary wave may be slowed by discreteness, impurities, and interaction with the environment and its speed may soon drop below the minimum value necessary for its existence. However, certain similar two-component excitations discussed in [48] proved to be stable or at least very long-living. This problem is an interesting subject worthy of further study, both analytical and numerical.

The results presented in this paper will be useful for the correct description of the metastable state decay in a discrete system. The problem is also of interest within the field of solid state physics [49], where discreteness certainly plays a significant role.

ACKNOWLEDGMENTS

P. Machnikowski was supported by the Polish State Committee for Scientific Research under Grant No. 2 P03B 089 14 and by the Foundation for Polish Science.

APPENDIX

Let us reiterate that the analysis of small oscillations around the kink solution in a symmetric potential [29] leads to the Schrödinger-type equation (6) with the Pöschl-Teller potential (10). For an on-site potential close to the symmetric one, i.e., $B^2-B_0^2 \ll 1$, the potential $V(\zeta)$ in Eq. (6) is close to two separated Pöschl-Teller wells, each of the form (10), as shown in Fig. 2. There is a solution to Eq. (6) with $\lambda^2=0$ and one solution with a lower eigenvalue that we are going to find. The lowest eigenlevels may be treated as a Wenzel-Kramers-Brillouin (WKB) pair. Without much inaccuracy one can take the Pöschl-Teller level $\lambda^2=0$ as the original one, instead of the zero-order WKB (Bohr-Sommerfeld) result for one well. The formula for the split between the levels then reads

$$\Delta(\lambda^2)=\frac{1}{2}\left[\int_{\zeta_i}^{\zeta_o}\frac{d\zeta}{\sqrt{\lambda^2-V(\zeta)}}\right]^{-1}\exp\left[\int_{-\zeta_i}^{\zeta_i}\sqrt{V(\zeta)-\lambda^2}d\zeta\right]$$

(limits of integration are shown in Fig. 2).

Although the integrals appearing in this formula may be calculated explicitly in terms of elliptic functions, it is much simpler, and accurate enough, to calculate the first integral as in a single PT well. Putting $\lambda^2=0$, one has

$$\int_{\zeta_i}^{\zeta_o}\frac{d\zeta}{\sqrt{\lambda^2-V(\zeta)}}\approx\int_{-\zeta'}^{\zeta'}\frac{d\zeta}{\sqrt{\frac{3}{2}\cosh^{-2}\frac{\zeta}{2}-1}}=2\pi,$$

where ζ' is a turning point for a symmetric PT potential.

As for the integral in the exponent, note that for a large enough separation of wells, increasing a by Δa results in increasing the integral by $2\Delta a$. Hence,

$$\int_{-\zeta_i}^{\zeta_o}\sqrt{V(\zeta)}d\zeta=S_0+2a.$$

Here S_0 is a constant and may be found numerically to be $S_0=1.8\pm0.1$. The value of ζ_i may be found from the condition $3u^2(\zeta_i)-2Bu(\zeta_i)+1=0$. The inner turning point corresponds to the solution $u(\zeta_i)=u_+=[B+\sqrt{B^2-3}]/3$. Thus, $\cosh\zeta_i=a/u_+-b$. Assuming that $B^2=B_0^2+\varepsilon^2$, we have $a\approx3/\varepsilon$, $b\approx B_0/\varepsilon+\varepsilon/(2B_0)$, and

$$u_+=\frac{1}{3}\left[B_0+\sqrt{B_0^2-3}+\frac{1}{2B_0}\varepsilon^2+\frac{1}{2\sqrt{B_0^2-3}}\varepsilon^2\right].$$

Inserting $B_0^2=9/2$ and keeping the leading terms we get $e^{\zeta_i}\approx2\cosh\zeta_i\approx(6\sqrt{2}-3\sqrt{6})\varepsilon^{-1}$. This leads to the split between the levels and, since the upper one is $\lambda^2=0$, to the lowest eigenvalue,

$$\lambda_0^2=-\frac{1}{4\pi}e^{-S_0}\frac{7+4\sqrt{3}}{3}\varepsilon^2.$$

Using the value of S_0 estimated above, one gets for the bell shape's lifetime

$$|\lambda_0|^{-1}\approx2\sqrt{\frac{3\pi}{7+4\sqrt{3}}}\frac{1}{\sqrt{B^2-B_0^2}}e^{0.9}.$$

[1] A. S. Davydov, *Solitony v Moliekuliarnykh Sistiemakh* (Naukova Dumka, Kiev, 1988) [*Solitons in Molecular Systems* (Reidel, Dordrecht, 1990)].
[2] A. Gordon, Physica B & C **146**, 373 (1987).
[3] S. Koshihara, Y. Tokura, K. Takeda, and T. Koda, Phys. Rev. B **52**, 6265 (1995).
[4] K. Koshino and T. Ogawa, J. Phys. Soc. Jpn. **67**, 2174 (1998).
[5] T. Dauxois, M. Peyrard, and A. R. Bishop, Phys. Rev. E **47**, 684 (1993).
[6] G. Gaeta, C. Reiss, M. Peyrard, and T. Dauxois, Riv. Nuovo Cimento **17**, 1 (1994).
[7] J. A. Krumhansl and J. R. Schrieffer, Phys. Rev. B **11**, 3535 (1975).
[8] J. F. Currie, S. E. Trullinger, A. R. Bishop, and J. A. Krumhansl, Phys. Rev. B **15**, 5567 (1977).
[9] V. G. Makhankov, Phys. Rep. **35C**, 1 (1978).
[10] M. A. Collins, A. Blumen, J. P. Currie, and J. Ross, Phys. Rev. B **19**, 3630 (1979).
[11] E. S. Kryachko, Solid State Commun. **65**, 1609 (1988).
[12] Y. Ishimori and T. Munakata, J. Phys. Soc. Jpn. **51**, 3367 (1982).
[13] J. Combs and S. Yip, Phys. Rev. B **28**, 6873 (1983).

[14] M. Peyrard and M. D. Kruskal, Physica D **14**, 88 (1984).
[15] C. Willis, M. El-Batanouny, and P. Stancioff, Phys. Rev. B **33**, 1904 (1986); P. Stancioff, C. Willis, M. El-Batanouny, and S. Burdick, *ibid.* **33**, 1912 (1986); R. Boesch, P. Stancioff, and C. R. Willis, *ibid.* **38**, 6713 (1988); R. Boesch and C. R. Willis, *ibid.* **39**, 361 (1989).
[16] A. Kwaśniewski, P. Machnikowski, and P. Magnuszewski, Phys. Rev. E **59**, 2347 (1999).
[17] T. Dauxois and M. Peyrard, Phys. Rev. Lett. **70**, 3935 (1993); T. Dauxois, M. Peyrard, and C. R. Willis, Phys. Rev. E **48**, 4768 (1993).
[18] J. F. Nagle, M. Mille, and H. J. Horowitz, J. Chem. Phys. **72**, 3959 (1980).
[19] S. N. Volkov and A. V. Savin, Ukr. Fiz. Zh. **37**, 498 (1992); S. N. Volkov, Phys. Lett. A **224**, 93 (1996).
[20] S. N. Volkov, J. Theor. Biol. **143**, 485 (1995).
[21] J. A. Gonzalez and J. A. Holyst, Phys. Rev. B **35**, 3643 (1987).
[22] A. Gordon, Physica B & C **150**, 319 (1988); Solid State Commun. **72**, 223 (1989).
[23] A. Gordon, Z. Phys. B: Condens. Matter **96**, 517 (1995).
[24] H. Metiu, K. Kitahara, and J. Ross, J. Chem. Phys. **64**, 292 (1976).
[25] P. Machnikowski and A. Radosz, Phys. Lett. A **242**, 313 (1998).
[26] C. W. Siders *et al.*, Nature (London) **286**, 1340 (1999).
[27] R. Rajaraman, *Solitons and Instantons* (North-Holland, Amsterdam, 1982).
[28] R. Jackiw, Rev. Mod. Phys. **49**, 681 (1977).
[29] J. F. Currie, J. A. Krumhansl, A. R. Bishop, and S. E. Trullinger, Phys. Rev. B **22**, 477 (1980).
[30] G. Pöschl and E. Teller, Z. Phys. **83**, 143 (1933).
[31] L. Infeld and T. E. Hull, Rev. Mod. Phys. **23**, 21 (1951).
[32] H. Konwent, P. Machnikowski, P. Magnuszewski, and A. Radosz, J. Phys. A **31**, 7541 (1998).
[33] R. S. MacKay and S. Aubry, Nonlinearity **7**, 1623 (1994).
[34] S. Flach and C. R. Willis, Phys. Rep. **295**, 181 (1998).
[35] I. L. Bogolyubskii and V. G. Makhan'kov, Pis'ma Zh. Éksp. Teor. Phys. **24**, 15 (1976) [JETP Lett. **24**, 12 (1976)]; **25**, 120 (1977) [**25**, 107 (1977)].
[36] M. Gleiser, Phys. Rev. D **49**, 2978 (1994).
[37] E. J. Copeland, M. Gleiser, and H. R. Müller, Phys. Rev. D **52**, 1920 (1995).
[38] R. M. Haas, Phys. Rev. D **57**, 7422 (1998).
[39] R. Boesch, C. R. Willis, and M. El-Batanouny, Phys. Rev. B **40**, 2284 (1989).
[40] S. Flach and C. R. Willis, Phys. Lett. A **181**, 232 (1993).
[41] J. S. Langer, Ann. Phys. (N.Y.) **54**, 258 (1969).
[42] B. I. Ivlev and V. I. Mel'nikov, Phys. Rev. B **36**, 6889 (1987).
[43] T. Christen, Phys. Rev. E **51**, 604 (1995).
[44] C. Claude, Y. S. Kivshar, O. Kluth, and K. H. Spatschek, Phys. Rev. B **47**, 14 228 (1993).
[45] R. Boesch and M. Peyrard, Phys. Rev. B **43**, 8491 (1991).
[46] J. Xu and J. Huang, Phys. Lett. A **197**, 127 (1995); J. Xu and B. Zhou, *ibid.* **210**, 307 (1996).
[47] A. Gordon, J. Phys.: Condens. Matter **8**, 4855 (1996).
[48] L. I. Manevich, V. V. Smirnov, A. V. Savin, and S. N. Volkov, Usp. Fiz. Nauk **164**, 937 (1994).
[49] F. Marchesoni, C. Cattuto, and G. Costantini, Phys. Rev. B **57**, 7930 (1998).